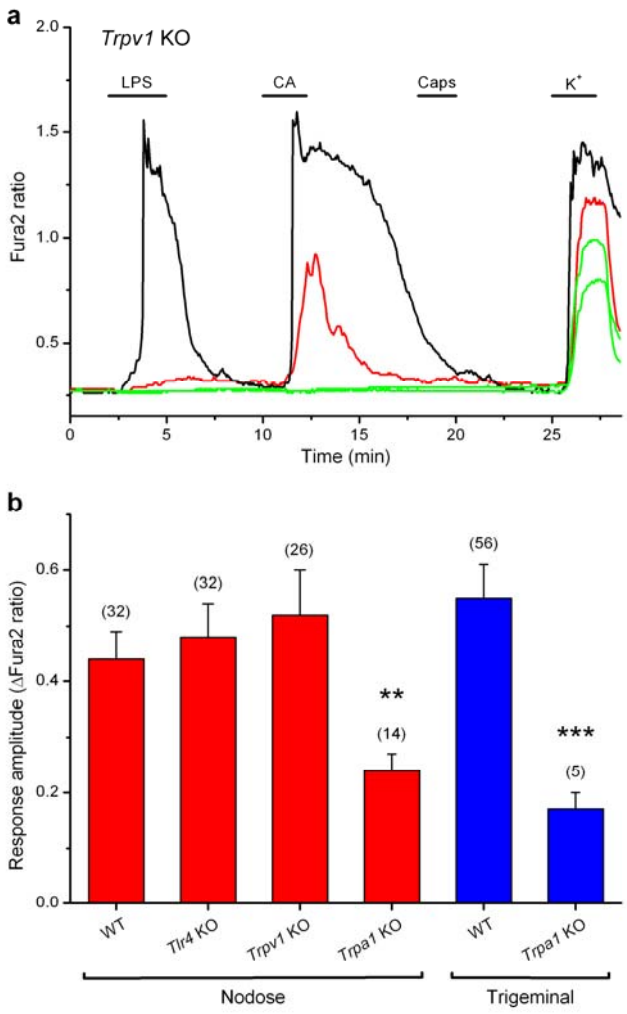

Supplementary Figure. 1. Intracellular Ca^{2+} responses to LPS are unaffected in *Tlr4* and *Trpv1* KO mice. (**a**) Representative example of the effect of *E. coli* LPS (10 µg/ml) on $[Ca^{2+}]_i$ in nodose ganglion neurons from *Trpv1* KO mice. Neurons were also stimulated with cinnamaldehyde (CA, 100 µM), capsaicin (Caps, 100 nM) and 60 mM K. (**b**) Summary of the average ± s.e.m response amplitudes to LPS (10 µg/ml) in nodose and trigeminal sensory neurons derived from different mouse lines. The number of individual cells measured are indicated in parenthesis. Asterisks denote statistically significant difference in the amplitude of responses in *Trpa1* KO neurons with respect to the respective WT cells (** $p < 0.01$, *** $p < 0.001$, unpaired t-test).

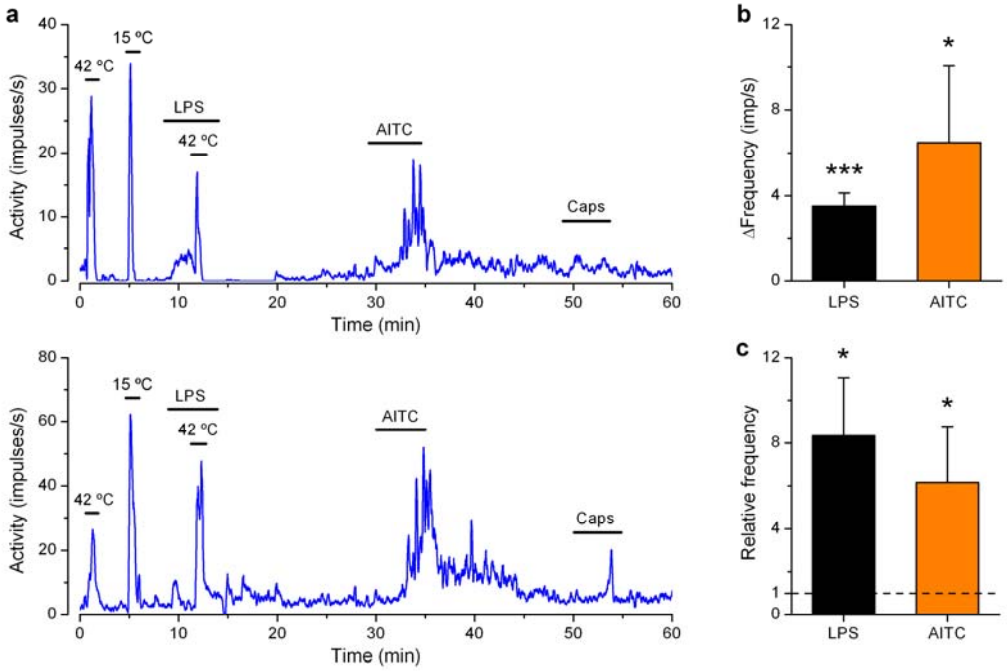

Supplementary Figure. 2. Activation of lingual nociceptors by LPS. (**a**) Two examples of the effect of LPS on the firing frequency of single polymodal nociceptor fibers innervating the mouse tongue. Heat (42 ºC), cold (15 ºC), LPS (200 µg/ml), AITC (100 µM) and capsaicin (5 µM) were applied during the periods indicated by the corresponding bars. (**b**) Average ± s.e.m. increase in firing frequency, measured at the peak, during application of LPS and AITC (* $p < 0.05$ and *** $p < 0.001$, paired t-test, n = 11). (**c**) Average ± s.e.m. firing frequency of LPS-sensitive single nociceptor fibers recorded in the presence of LPS or AITC, relative to the average value recorded in control (* $p < 0.05$, n = 11, paired t-test).

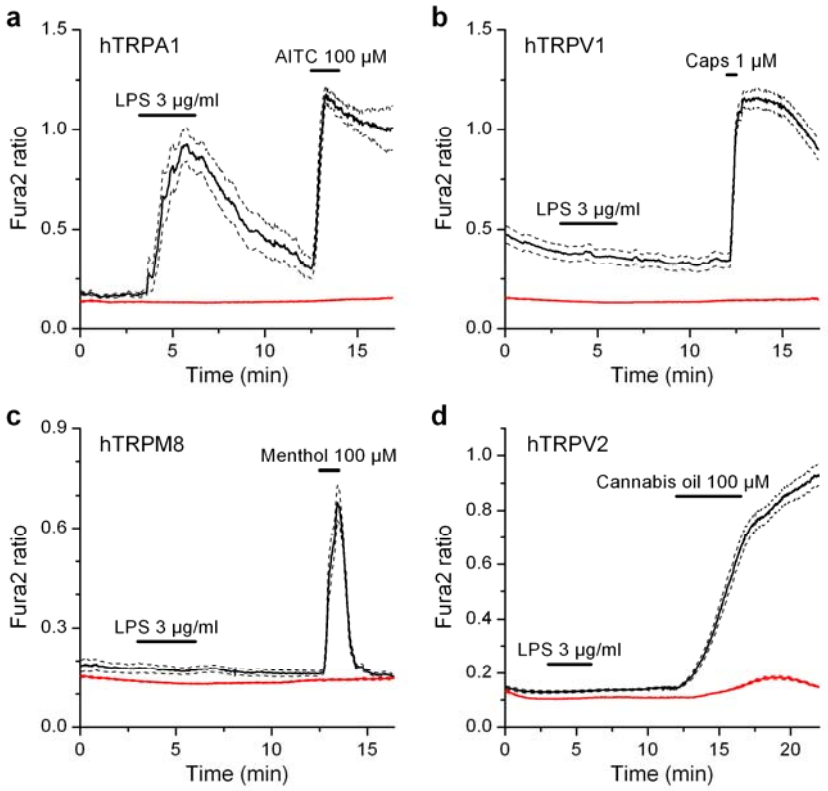

Supplementary Figure. 3. Effect of *E. coli* LPS on human thermoTRP channels expressed in sensory neurons. (**a**, **d, c** and **d**) Examples of the effects of LPS (3 µg/ml) on $[Ca^{2+}]_i$ levels in HEK-293 cells transfected with the human variant of (**a**) TRPA1, n = 35 (**b**) TRPV1, n = 77 (**C**) TRPM8, n = 41 and (**d**) TRPV2, n = 71. Following washout of LPS, the cells were stimulated with the respective canonical ligands, AITC, capsaicin (Caps), menthol and cannabis oil. The solid black trace and the dashed lines show the mean and ± s.e.m respectively. The red lines show the average response in non-transfected cells (n > 20).

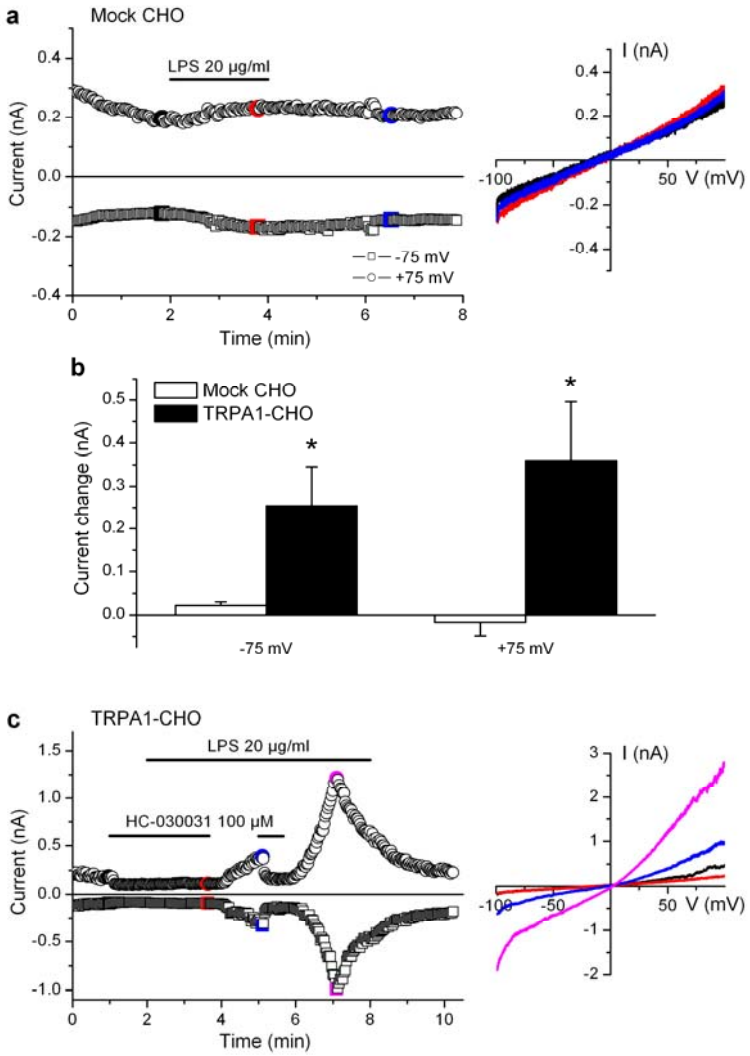

Supplementary Figure. S4. Effects of *E. coli* LPS on TRPA1 currents studied by whole-cell patch-clamp. (**a**) Lack of significant effect of LPS on the current amplitudes measured at -75 and at +75 mV in non-transfected CHO cells. On the right, representative I-V curves from the same experiment, obtained before (black), during (red) and after (blue) LPS application. (**b**) Average ± s.e.m current increment produced by LPS (20 µg/ml) in mTRPA1 CHO cells (n = 6) and control, untransfected, CHO cells (n = 7) measured at two holding potentials. The increments were statistically significant ($p<0.05$, unpaired t-test) (**c**) Time course of TRPA1 current response to LPS and the TRPA1 inhibitor HC-030031 (HC) monitored at -75 and +75 mV. Pre-application of HC-030031 prevented the increase of the current during LPS application. On the right, representative I-V curves from the same experiment. The color of each current trace corresponds to colored symbol on the left.

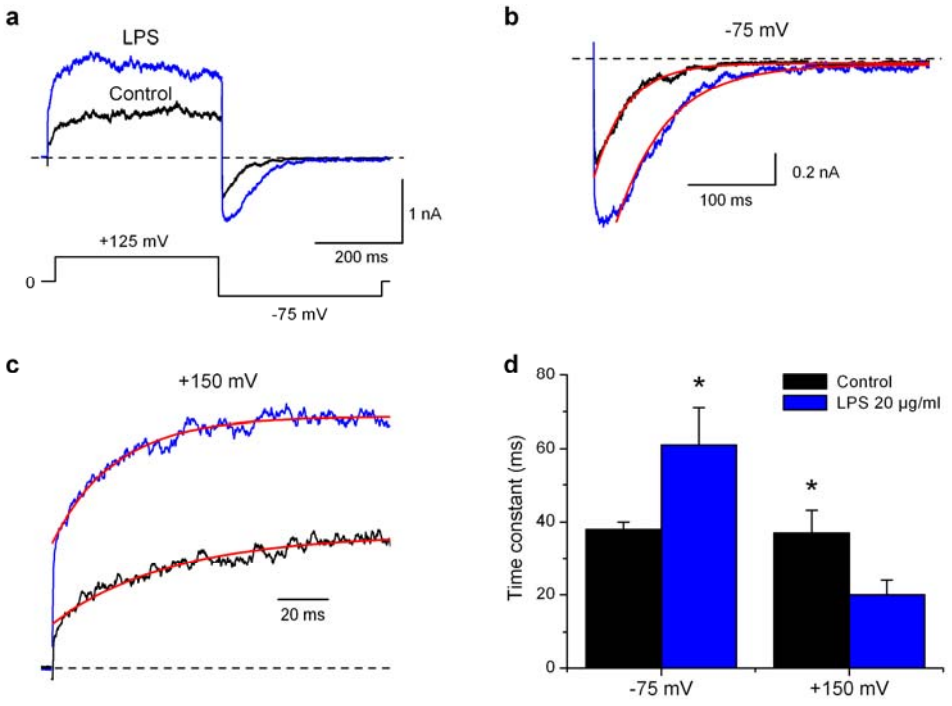

Supplementary Figure. 5. Effects of *E. coli* LPS on the gating kinetics of TRPA1. (**a**) Mouse TRPA1 currents recorded in CHO cells in response to a double-pulse voltage protocol in control solution (black) and in the presence of *E. coli* LPS (20 µg/ml) (blue trace). (**b**) Inward tail current in control solution (black) and in 20 µg/ml LPS (blue trace) measured at -75 mV following a step to +125 mV. The time courses of the currents were fitted with single mono-exponential functions (time constant of 38 and 58 ms respectively). (**c**) Time course of currents in control solution (black) and in 20 µg/ml LPS (blue trace) during a step to +150 mV. The time courses of the currents were fitted with single mono-exponential functions (time constant of 48 and 25 ms respectively). (**d**) Average ± s.e.m time constants (n = 6) obtained from mono-exponential fits to the time course of current relaxation at different voltages in control (black) and LPS (blue). The difference was significant ($p < 0.05$, paired t test).

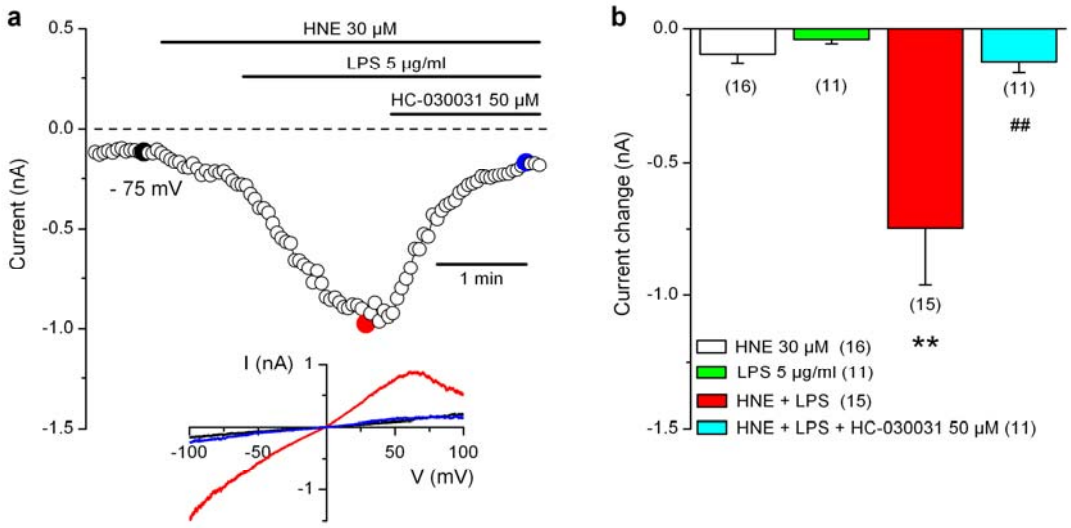

Supplementary Figure. 6. The endogenous TRPA1 agonist 4-hydroxynonenal (HNE) potentiates responses to low concentrations of LPS. (**a**) Time course of whole cell current at -75 mV in a mTRPA1-expressing cell during application of HNE (30 µM) and LPS (5 µg/ml). The current activated by both agonists was fully blocked by HC-030031. The inset shows the I-V relationship of the current at the time points marked by the different colors. (**b**) Summary of mean ± s.e.m current activation at -75 mV by HNE, LPS or both agonist co-applied, and the blocking effect of HC-030031. Current increase in HNE + LPS, measured isochronally, is significantly larger (**) than current increase to each agonist alone ($p<0.01$, one way ANOVA and Bonferroni posthoc correction). HC-030031 inhibited the current (##) induced by HNE + LPS by 84.2 ± 4.0% ($p<0.01$; unpaired t-test). Numbers in parenthesis indicate cells for each experimental group.

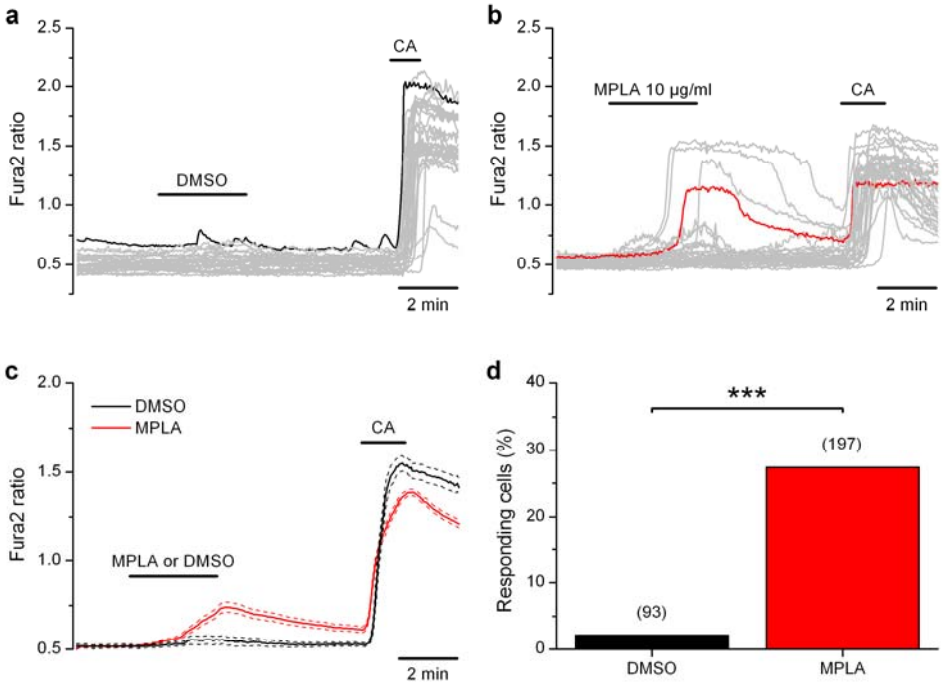

Supplementary Figure S7. Synthetic monophosphoryl Lipid A (MPLA) activates TRPA1 channels. Application of vehicle (DMSO) (**a**) had no effect while application of MPLA (**b**) produced a clear activation of TRPA1-expressing CHO cells (30 cells per field). (**c**) Average (solid lines) ± s.e.m (broken lines) time course of response to DMSO (n = 46) or MPLA (n = 197) and 100 µM cinnamaldehyde (CA). (**d**) The percentage of TRPA1-expressing cells (total number in parenthesis) responding to MPLA or DMSO. The difference in proportions was significantly different ($p < 0.001$ Fisher's exact test).

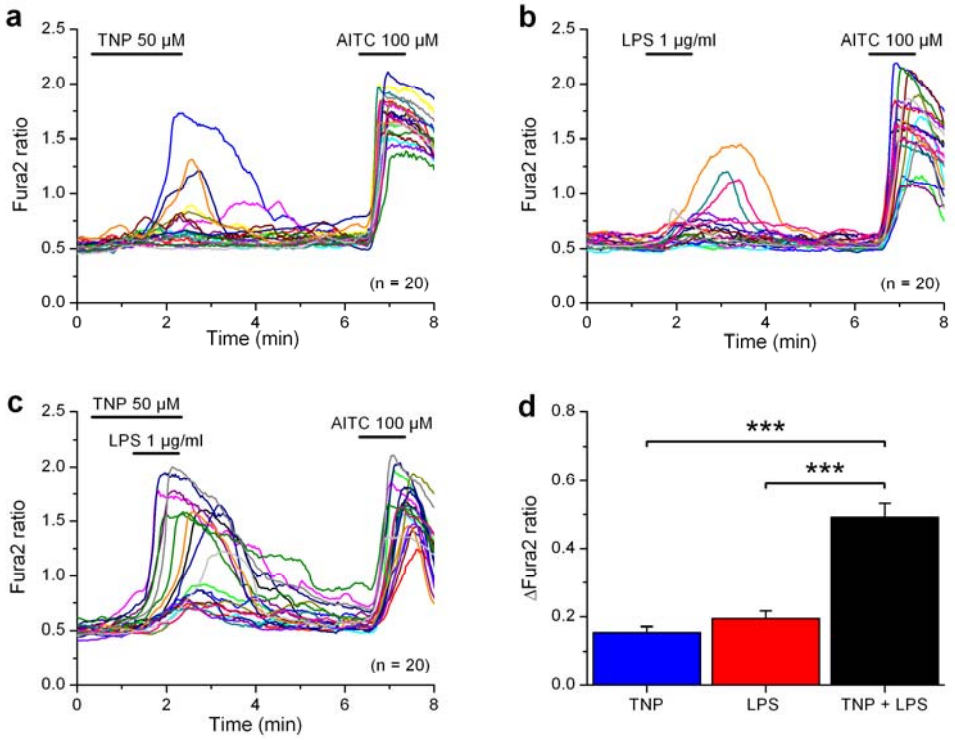

Supplementary Figure. 8. The membrane crenator trinitrophenol potentiates responses to *E. coli* LPS in mTRPA1 cells. (**a, b** and **c**) Time course of $[Ca^{2+}]_i$ elevation in mTRPA1 cells in response to trinitrophenol (50 µM), LPS in control solution (1 µg/ml) and LPS in the presence of trinitrophenol. (**d**) Bar charts representing the average amplitude ± s.e.m. of responses to TNP (n = 157), LPS (n = 122) and TNP plus LPS (n = 135). *** indicates $p < 0.0001$; one way ANOVA with Bonferroni post-hoc test.

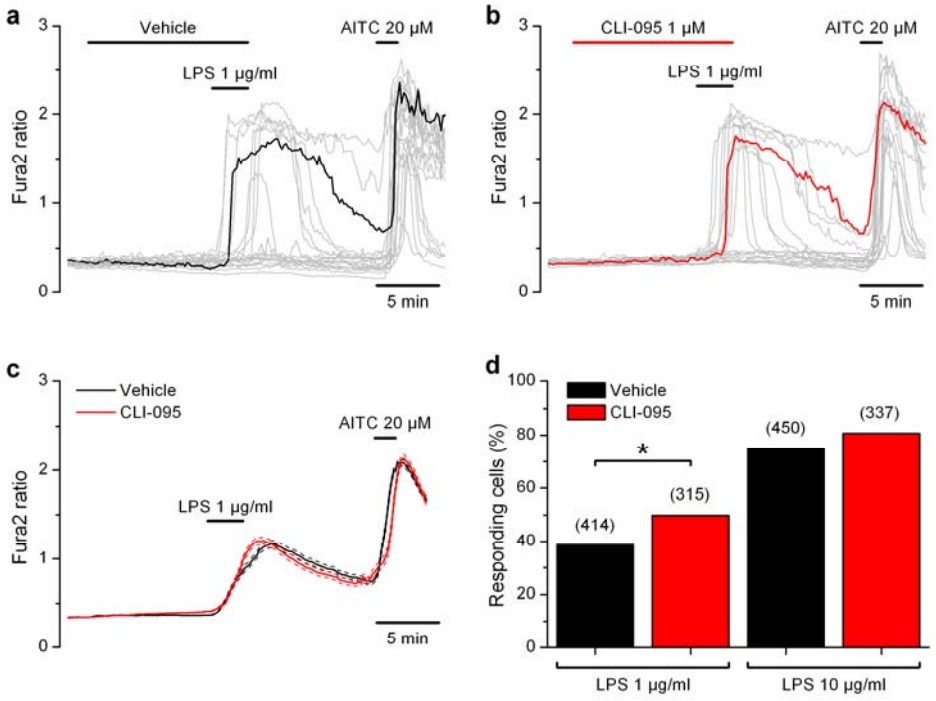

Supplementary Figure 9. Inhibition of TLR4 signaling does not prevent TRPA1 activation by LPS. Preincubation for 10 minutes with vehicle (**a**) or CLI-095 (**b**) did not affect the response to low-doses of LPS in TRPA1-expressing CHO cells. (**c**) Average (solid) ± s.e.m. (broken lines) time course of response to LPS and AITC in cells pretreated with vehicle (n = 20) or CLI-095 (n = 20). Note the nearly identical amplitude of both responses. (**d**) The percentage of TRPA1-expressing cells (number in parenthesis) responding to 1 μg/ml LPS increased slightly during CLI-095 pretreatment (Fishers's exact test).

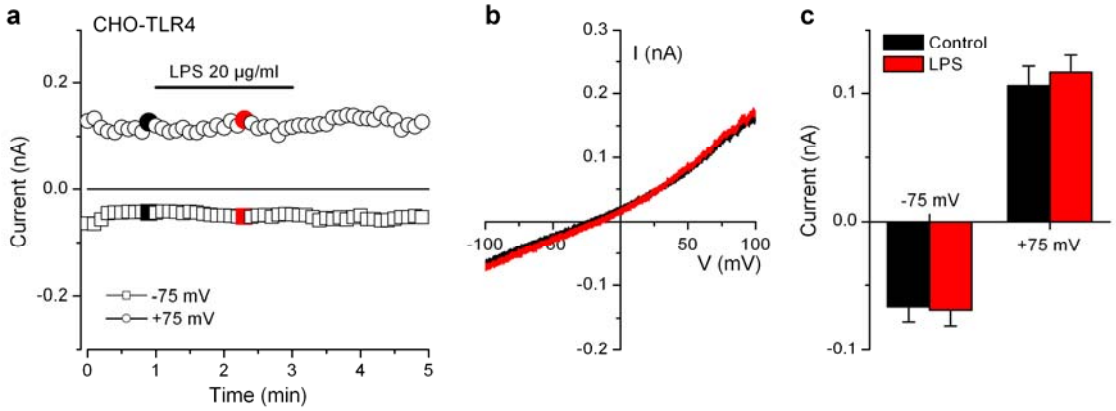

Supplementary Figure. 10. Lack of effects of *E. coli* LPS on ionic currents in CHO cells transfected with human TLR4 studied by whole-cell patch-clamp. (**a**) Time course of whole-cell current measured at -75 and at +75 mV. (**b**) Representative I-V curves from the same experiment, obtained before (black) and during (red) LPS application. (**c**) Average ± s.e.m current, measured at +75 mV in control and during application of LPS (20 µg/ml) in hTLR4 CHO cells (n = 8, p = 0.6, paired t-test).

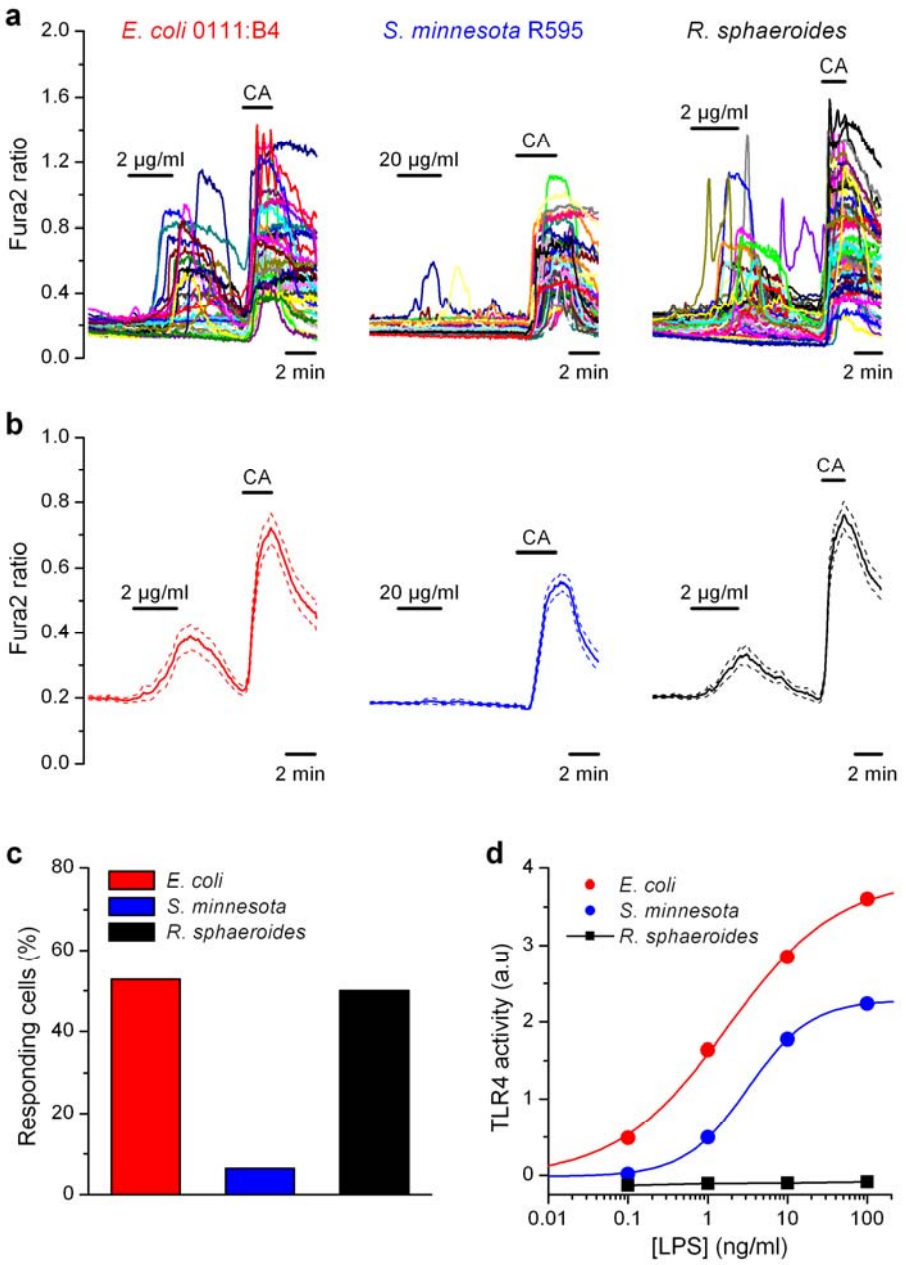

Supplementary Figure. 11. Differential effects of ultrapure preparations of different LPS forms on TRPA1 and TLR4 activity. (**a**) Calcium responses of mTRPA1 cells to ultrapure preparations of LPS. Note that responses to *Salmonella minnesota* LPS are very rare, despite using a 10 times higher concentration. (**b**) Mean (solid) ± s.e.m (dashed) response amplitude, calculated for the same fields as panel **a** (n > 90 cells for each field). (**c**) Cells responding to LPS, calculated as percentage of cinnamaldehyde (CA) responses in the same fields. (**d**) Effects of same forms of ultrapure LPS on TLR4 signaling. TLR4 activity was monitored on HEK-Blue-hTLR4 cells (InvivoGen). Cells were incubated with different concentrations of LPS for 18 hours. Average results (n=6) have been normalized to values obtained with endotoxin free water. Errors bars (s.e.m.) are smaller than diameter of data points. As expected, *E. coli* and *S. minnesota* LPS induced strong TLR4 activity. On the other hand, note the lack of activity of LPS extracted from *R. sphaeroides* on TLR4, in contrast with its clear effects on TRPA1 activation.

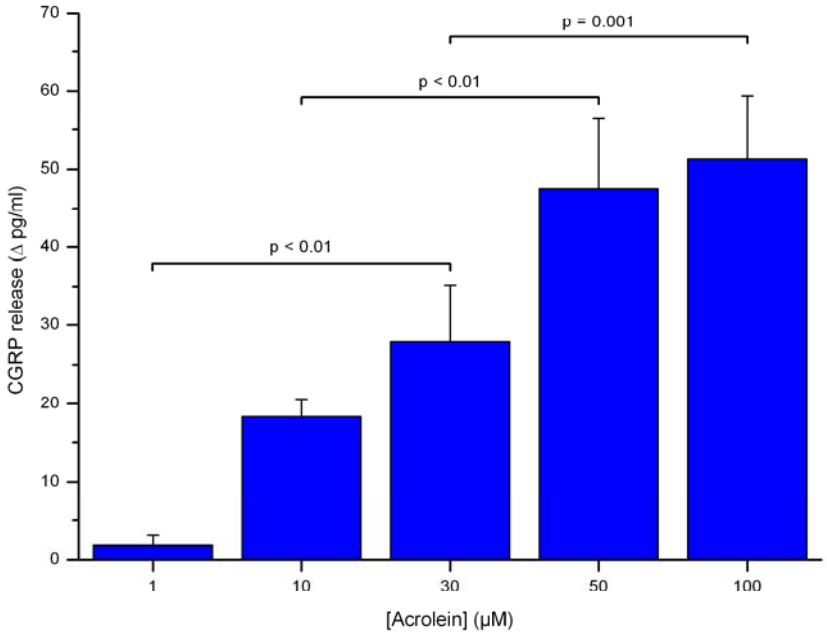

Supplementary Fig. 12. Dose-dependent release of CGRP from the mouse trachea by acrolein. Mouse trachea halves were incubated for 5 minutes with different concentrations of acrolein. The CGRP content of the incubation fluid was measured using a commercial enzyme immunoassay kit. Data represent the mean ± s.e.m. (n > 6 for each concentration). The p values were obtained by one way ANOVA followed by Least Significance Difference Test.

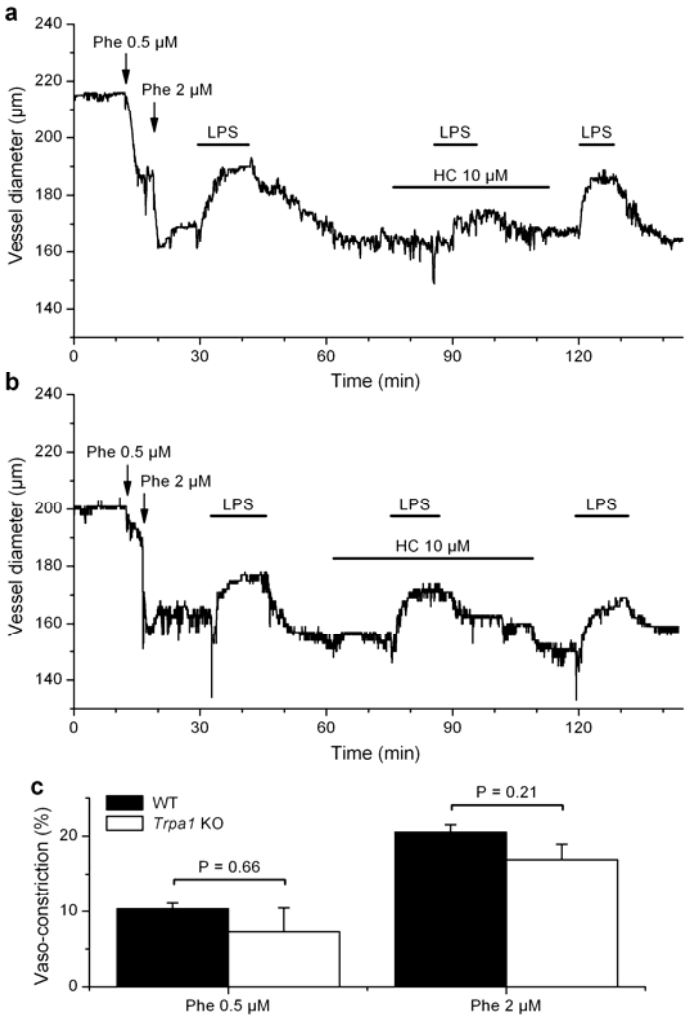

Supplementary Figure. 13. A component of the vasodilatory response to LPS is mediated by TRPA1. Representative examples of the effect of *E. coli* LPS (100 µg/ml) perfusion on mesenteric artery diameter from WT (**a**) and *Trpa1* KO (**b**) mice in control condition, in the presence of HC-030031 (10 µM) and after wash. Arteries pre-contracted with the alpha1 adrenergic agonist phenylephrine (2 µM). (**c**) The vasoconstrictor effect of phenylephrine is not altered in *Trpa1* KO mice. Data are mean ± s.e.m of 7-9 arteries (Phe 0.5 µM) and 6-8 arteries (Phe 2 µM). The p value was obtained in an unpaired, 2-tail, t-test.

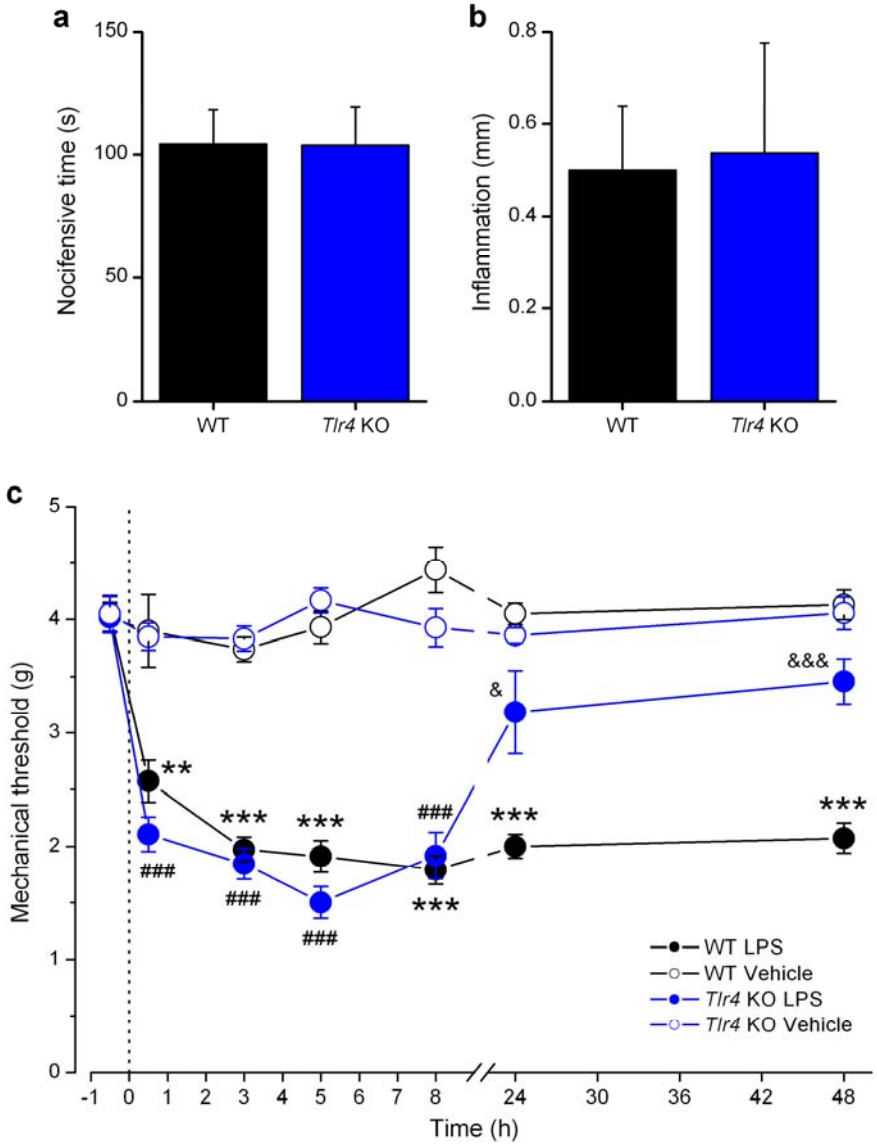

Supplementary Figure. 14. Genetic ablation of *Tlr4* does not influence the acute nocifensive and inflammatory responses to LPS. (**a**) Mean ± s.e.m. nocifensive response and (**b**) Mean ± s.e.m. acute local inflammation produced by intraplantar LPS injection of *E. coli* LPS (5 µg/µl in 10 µl) in WT (n = 6) and *Tlr4* KO animals (n = 6). (**c**) Mechanical paw withdrawal threshold to mechanical stimulation before (t = -0.5 h) and at several time points after intraplantar injection of LPS (5 µg/µl) in WT (n = 6) and *Tlr4* KO (n = 6) animals. Vehicle was saline injected in the contralateral paw of the same animals. The asterisks and ### symbols indicate the differences with respect to baseline (one way ANOVA with Bonferroni's correction; double symbols $p < 0.01$ and triple symbols $p < 0.001$). The differences between WT and KO mice are denoted by the symbols & ($p < 0.05$) and && ($p < 0.01$) (unpaired two-tailed Student's t-test).

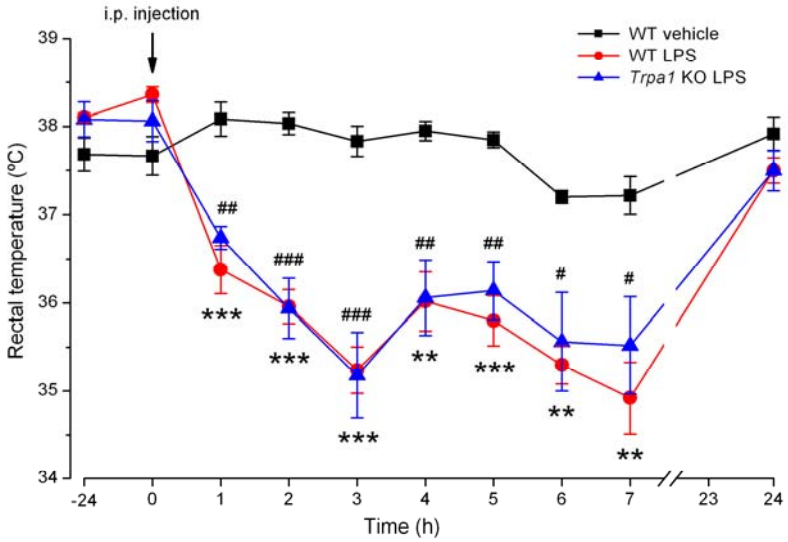

Supplementary Figure. 15. TRPA1 does not participate in the body temperature (Tb) response to LPS in a cool environment. Effect of an i.p. injection LPS (3 mg/kg in saline) on Tb (mean ± s.e.m.) in wildtype (n = 6) and *Trpa*1 KO mice (n = 5). Responses were compared to i.p. saline injections in wildtype mice (n = 6) (ANOVA with Bonferroni post-hoc test). # compares responses to vehicle in wildtype to responses to LPS in *Trpa*1 KO mice. The asterisks (*) compare responses to vehicle and LPS in wildtype mice.

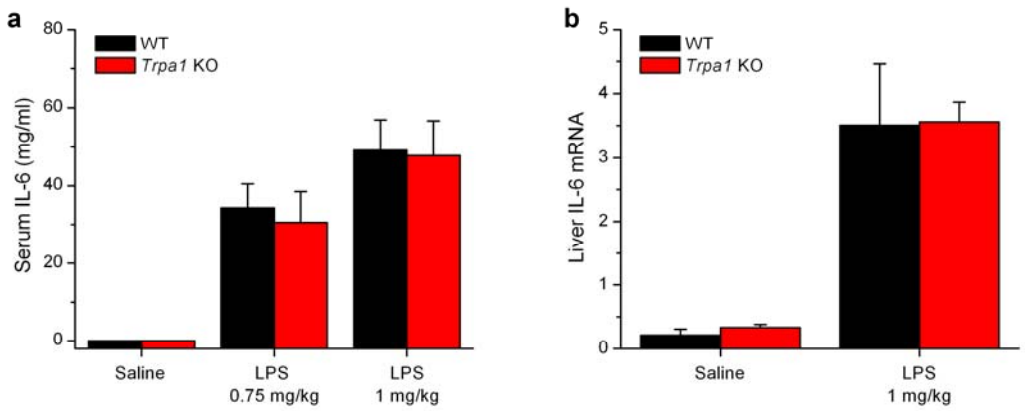

Supplementary Figure. 16. Elevation of circulating IL-6 levels by LPS are not affected in *Trpa1* KO mice. (**a**) Basal serum IL-6 levels were undetectable and increased dose-dependently after 1 hour of an i.p. LPS injection in WT (n = 6) and *Trpa1* KO (n = 6) mice. (**b**) Liver mRNA levels increased similarly in WT (n = 3) and *Trpa1* KO (n = 3) mice following the i.p. LPS injection. Data are mean ± s.e.m.